High-resolution MS/MS characterization of steroid fragmentation profiles for structural elucidation

Nathan Ghafari, Lekha Sleno*

Bioanalytical Mass Spectrometry Research Group, Chemistry Department, University of Quebec in Montreal (UQAM), Montreal, QC, Canada

**Corresponding author: sleno.lekha@uqam.ca*

Abstract

The analysis of steroids by liquid chromatography - tandem mass spectrometry (LC-MS/MS) is associated with several analytical challenges, including difficulty in confirming their structures in complex samples, due to structural similarities. Collision-induced dissociation (CID) is commonly employed but many aspects of the fragmentation behavior of steroids remain unexplored. In this study, we report the systematic high-resolution MS/MS characterization of 33 endogenous steroid standards analyzed using a microLC-HRMS/MS workflow on a quadrupole-time-of-flight platform in positive mode, while varying collision energies, for their native forms and Girard P (GP) derivatives. For underivatized steroids, intermediate collision energies produced the most interpretable spectra, enabling the identification of many class-specific diagnostic ions. The multiple collision energies tested revealed strong dependence of both precursor persistence and diagnostic fragment presence related to structural features present in the steroids. Girard P derivatization increased signal intensities and altered their chromatographic retention, with the signal enhancement depending on the presence of specific structural features. Higher collision energies applied to GP-derivatized steroids revealed diagnostic fragments, useful for structural characterization. Fragmentation patterns and collision energy-dependent profiles provide increased confidence for steroid structural classification and isomer discrimination.

Keywords

Steroids; LC-HRMS/MS; CID fragmentation; Derivatization; Diagnostic fragment ions

Introduction

Endogenous steroids constitute a large family of metabolites that share a common four ring backbone but differ through variations in oxidation, double-bond positions, and stereochemistry[1]. These small structural changes generate many closely-related molecules with similar physicochemical properties[2]. As a result, distinguishing individual steroids requires analytical approaches to provide detailed information on their structure such as tandem mass spectrometry (MS/MS). Understanding how these structural differences influence chromatographic and fragmentation behavior is essential for the reliable characterization of steroids especially in the context of complex biological matrices.

Steroids present several analytical challenges, particularly when investigated by LC-MS/MS, as many have structural isomers, some of which exhibit distinct biological roles[3–5], and thus need to be differentiated. Several studies have attempted to address this issue through optimized chromatographic separations[6–8] or by introducing additional dimensions of separation, such as ion mobility[9–14]. Another issue is the low levels of many endogenous steroids in biological matrices. Their low concentration often requires extensive sample preparation, including concentration steps or derivatization procedures designed to enhance ionization efficiencies and reduce matrix effects. Such strategies are frequently employed to improve chromatographic behavior and enhance ionization, typically through the introduction of functional groups, such as permanently charged or easily ionizable moieties[15–20]. However, derivatization reagents commonly used for carbonyl-containing steroids like hydrazine-based reagents often produce molecules that undergo a dominant and non-informative loss corresponding to the derivatizing moiety[21], thereby reducing the structural information in the resulting MS/MS spectra.

One of the most common solutions to sensitivity limitations for steroid analysis has been the use of targeted multiple reaction monitoring (MRM) workflows[22–25]. Although powerful, this approach is associated with many restrictions. First, identification is limited by the predefined transition list, removing the potential of detecting unexpected or unmonitored steroids. Second, many isomeric steroids share identical precursor and product ions, requiring baseline chromatographic separation prior to MRM detection, otherwise structural differentiation cannot be achieved. Another limitation of using low-resolution MRM analysis on triple quadrupole platforms is the absence of exact mass information for precursor and fragment ions. High-resolution MS/MS enables discrimination between steroid fragments with identical nominal masses, which cannot be resolved at lower resolution. Their chemical structures contribute to the complexity of steroid analysis, their common four-ring backbone and prevalent functional groups (ketones and secondary alcohols) provide relatively poor protonation sites under electrospray conditions. Moreover, many steroids can undergo in-source fragmentation often from the loss of a neutral water molecule, and the conserved core structure frequently yields nonspecific fragments with limited structurally diagnostic value. These factors highlight the need for detailed high-resolution MS/MS characterization of steroid fragmentation behavior to help distinguish structurally informative features for confident steroid identification. Some recent

studies have employed machine learning or automated workflows for helping elucidate structures of steroids[26] or bile acids[27].

In this study, we analyzed a panel of 33 endogenous steroid standards, in their native forms and after carbonyl derivatization with Girard P, using an untargeted microLC-HRMS/MS workflow. The aim was to characterize their fragmentation behavior at different collision energies and evaluate how the derivatization influences chromatographic separation and fragmentation. Particular attention was given to diagnostic fragment ions that enable differentiation between major steroid structural classes and isomers.

Material and methods

Chemical and reagents

Methanol (MeOH), acetonitrile (ACN), formic acid, acetic acid and isopropanol (IPA) were all from Sigma Aldrich (Oakville, ON, Canada). Girard P reagent (1-(hydrazinocarbonylmethyl)pyridinium chloride) was purchased from TCI Chemicals (Portland, OR, USA). Nanopure water was produced using a Millipore Synergy UV purification system (Billerica, MA, USA). Estrone (E1), estradiol (E2), testosterone (T), epiandrosterone (EpiA), pregnenolone (P5), 11-α-hydroxyprogesterone (11α-OHP), cortisone (E), dehydroepiandrosterone (DHEA), dehydrotestosterone (DHT), progesterone (P4), 11-deoxycorticosterone (11-DOC), 11-dehydrocorticosterone (11-DHC), corticosterone (CORT), and cortisol (F) were purchased from Sigma-Aldrich (Oakville, ON, Canada). ß-dihydroprogesterone (5ß-DiHP4), deoxycortisol (S), ß-dihydrocorticosterone (5ß-DiHCORT), aldosterone (ALD), androstenedione (A4), 11-ketotestosterone (11-KT), α-dihydroprogesterone (5α-DiHP4), α-dihydrocorticosterone (5α-DiHCORT), estriol (E3), 3α-androstanediol (3α-Diol), 7α-hydroxy-dehydroepiandrosterone (7α-OH-DHEA), 17α-hydroxyallopregnanolone (17α-OH-AlloP), androsterone (AN), 7ß-hydroxy-dehydroepiandrosterone (7ß-OH-DHEA), 17ß-hydroxyallopregnanolone (17ß-OH-AlloP), 16α-hydroxy-dehydroepiandrosterone (16α-OH-DHEA), 17α-hydroxypregnenolone (17α-OH-P5), tetrahydro-deoxycorticosterone (THDOC), and allopregnanolone (AlloP) were obtained from Steraloids (Newport, Rhode Island, USA).

Sample preparation and Evotips loading procedure

Steroid standards were prepared in 7 different mixes (to avoid mixing isomers) in 25% MeOH at a concentration of 100 ng/mL. For each mix, 20 µL were loaded onto Evotips (Evotip Pure, Evosep, Odense, Denmark) that were conditioned prior to use. Tips were equilibrated with 20 µL of mobile phase B (0.1% formic acid in ACN) and centrifuged at 800 g for 1 min to pass liquid through (at each step of added solution), followed by immersing tips in isopropanol (10s), and rinsing with 20 µL of mobile phase A (0.1% formic acid in water). A 20 µL aliquot of each standard mix was loaded onto the tips, followed by a wash step with MP A and further addition of 200 µL on top of the tips, with the tips immersed in MP A prior to analysis.

Girard P derivatization

For Girard P derivatization, 200 µL of each steroid mixture was dried using a vacuum concentrator (Fisher Scientific, Mississauga, ON, Canada), then resuspended in 150 µL of methanol containing 10% acetic acid, after which 50 µL of a Girard P reagent solution (10 mg/mL in 50% acetonitrile) was added. Samples were mixed and allowed to react for 10 min at 60 °C. After derivatization, solvents were removed by nitrogen-assisted evaporation, and the samples were reconstituted in 200 µL 25% methanol. The derivatized standard mixes obtained were loaded on Evotips (as above).

LC-HRMS/MS analysis

Chromatographic separation was achieved with an Evosep One LC system using the "high organic" SPD 100 (100 sample per day) method, ramping mobile phase B from 10% to 100% at 1.5 µL/min on a Evosep Endurance C18 column (8 cm × 0.1 mm, 3 µm). The LC method duration was 11.5 min, with a total of 14 min between samples. A ZenoTOF 7600™ QqTOF (Sciex, Concord, ON, Canada) equipped with OptiFlow electrospray ion source was used in positive mode. The following source conditions were used: source temperature of 150 °C, curtain gas at 35 psi, GS1 10 psi, GS2 25 psi, and a spray voltage of 4.5 kV. TOF-MS spectra were collected from *m/z* 270–625 with an accumulation time of 0.1 s. TOF-MS/MS were acquired in MRM^{HR} acquisition mode by targeting each precursor ion (at unit resolution of the quadrupole with isolation width of 0.7 Da) and detecting fragment ions from *m/z* 40 - 400 with an accumulation time between 0.012 and 0.020 s each, depending on the number of MRM^{HR} experiments in each method, with total cycle times ranging from 0.965 to 1.065 s. Each precursor was fragmented at multiple collision-offset voltages (CE) ranging from 10 to 60 V, at 5 V intervals. The details of the nine MRM^{HR} methods used in this study are outlined with the list of targeted precursors in **Supplementary Data (Table S1).**

Data processing

All acquired LC–MS/MS data were visualized and extracted ion chromatograms generated using PeakView 2.2 software, with Masterview (Sciex). The exact mass of each precursor was measured within 5 ppm. Underivatized steroids were detected as protonated molecules, whereas GP-derivatized steroids produced permanently charged species due to the presence of the reagent's quaternary amine, therefore precursors were detected as M^+ ions.

High-resolution MS/MS data were extracted from the top of each LC peak of interest with SciexOS-Q 2.0.1 to compile peak heights of precursors and fragments at 11 different collision energies for each steroid. Chemical formulas for individual fragment ions were subsequently assigned based on their exact masses (within a maximum of 10 ppm), restricted to the specific precursor ion formula, using a modified version of a Python-based package (find-mfs)[28].

Results and discussion

All steroid standards analyzed in this study belong to classical endogenous categories such as androgens, progestogens, corticoids, and estrogens. However, although biologically relevant, these categories are not necessarily informative from a structural or analytical perspective, as steroids within the same biological category can exhibit substantial differences in A-ring functionality, oxidation state, and unsaturation. Because CID fragmentation behavior is primarily impacted by molecular structure, all steroids investigated were therefore classified into six distinct structure-based categories (**Figure 1**). These categories were defined according to key structural features known to impact fragmentation patterns, such as A-ring groups, oxidation state or side chains, in agreement with existing literature on steroid structural classification[29–32]. Five structural categories primarily reflecting A-ring chemistry were used, complemented by an additional category for steroids with an alkyl side chain at the C17 position. A complete list of studied steroids, together with their assigned structural category and defining structural features, is provided in **Table 1**, with their individual structures shown in **Supplementary Data (Figure S1)**.

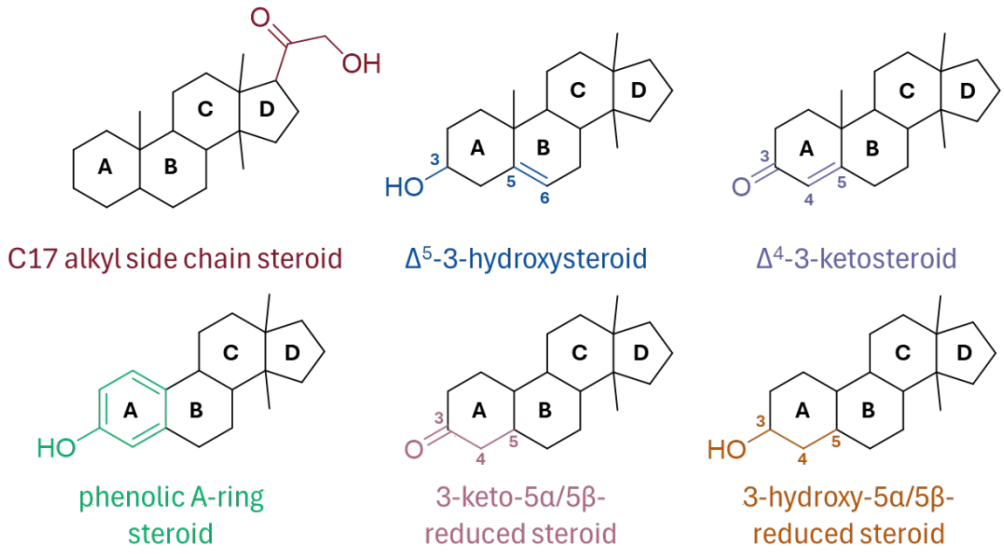

Figure 1. Structural categories of endogenous steroids studied in this work

The overlaid extracted ion chromatograms of the protonated molecules for the 33 studied steroids are provided in **Supplementary Data (Figure S2).** For several steroids, in-source fragmentation was observed, primarily corresponding to one or two water losses. In some cases, the dehydrated ion exceeded that of the intact precursor's intensity. This behavior is consistent with the presence of hydroxyls on a non-aromatic ring or side chain. Accordingly, both intact precursor and major in-source dehydration products were considered during precursor selection and subsequent MS/MS interpretation.

Table 1: Studied steroids with their associated characteristics and structural information

Name	Formula	$(MH)^+$	RT	Structural classification	Unsaturation (Δn)	R3	R11	R17
estrone (**E1**)	$C_{18}H_{22}O_2$	271.1693	8.4	phenolic A ring steroid	A ring	—OH	-	=O
estradiol (**E2**)	$C_{18}H_{24}O_2$	273.1849	7.8	phenolic A ring steroid	A ring	—OH	-	—OH
testosterone (**T**)	$C_{19}H_{28}O_2$	289.2162	8.0	Δ^4-3-ketosteroid	Δ^4	=O	-	—OH
epiandrosterone (**EpiA**)	$C_{19}H_{30}O_2$	291.2319	8.8	3-hydroxy-5α/5β-reduced steroid	-	—OH	-	=O
pregnenolone (**P5**)	$C_{21}H_{32}O_2$	317.2475	9.8	Δ^5-3-hydroxysteroid	Δ^5	—OH	-	$C(O)CH_3$
11-α-hydroxyprogesterone (**11α-OHP**)	$C_{21}H_{30}O_3$	331.2268	7.4	Δ^4-3-ketosteroid*	Δ^4	=O	—OH	$C(O)CH_3$
cortisone (**E**)	$C_{21}H_{28}O_5$	361.2010	5.7	Δ^4-3-ketosteroid*	Δ^4	=O	=O	—OH
dehydroepiandrosterone (**DHEA**)	$C_{19}H_{28}O_2$	289.2162	8.4	Δ^5-3-hydroxysteroid	Δ^5	—OH	-	=O
dihydrotestosterone (**DHT**)	$C_{19}H_{30}O_2$	291.2319	8.9	3-keto-5α/5β-reduced steroid	-	=O	-	—OH
progesterone (**P4**)	$C_{21}H_{30}O_2$	315.2319	9.8	Δ^4-3-ketosteroid	Δ^4	=O	-	$C(O)CH_3$
11-deoxycorticosterone (**11-DOC**)	$C_{21}H_{30}O_3$	331.2268	8.2	Δ^4-3-ketosteroid*	Δ^4	=O	-	$C(O)CH_2OH$
11-dehydrocorticosterone (**11-DHC**)	$C_{21}H_{28}O_4$	345.2060	6.5	Δ^4-3-ketosteroid*	Δ^4	=O	=O	$C(O)CH_2OH$
corticosterone (**CORT**)	$C_{21}H_{30}O_4$	347.2217	6.8	Δ^4-3-ketosteroid*	Δ^4	=O	—OH	$C(O)CH_2OH$
cortisol (**F**)	$C_{21}H_{30}O_5$	363.2166	5.6	Δ^4-3-ketosteroid*	Δ^4	=O	—OH	—OH
ß-dihydroprogesterone (**5ß-DiHP4**)	$C_{21}H_{32}O_2$	317.2475	10.4	3-keto-5α/5β-reduced steroid	-	=O	-	$C(O)CH_3$
deoxycortisol (**S**)	$C_{21}H_{30}O_4$	347.2217	7.8	Δ^4-3-ketosteroid	Δ^4	=O	-	OH + $C(O)CH_2OH$
ß-dihydrocorticosterone (**5ß-DiHCORT**)	$C_{21}H_{32}O_4$	349.2373	6.4	3-keto-5α/5β-reduced steroid*	-	=O	—OH	$C(O)CH_2OH$
aldosterone (**ALD**)	$C_{21}H_{28}O_5$	361.2010	5.2	Δ^4-3-ketosteroid*	Δ^4	=O	—OH	$C(O)CH_2OH$
androstenedione (**A4**)	$C_{19}H_{26}O_2$	287.2006	8.4	Δ^4-3-ketosteroid	Δ^4	=O	-	=O
11-ketotestosterone (**11-KT**)	$C_{19}H_{26}O_3$	303.1955	6.2	Δ^4-3-ketosteroid	Δ^4	=O	=O	—OH
α-dihydroprogesterone (**5α-DiHP4**)	$C_{21}H_{32}O_2$	317.2475	10.5	3-keto-5α/5β-reduced steroid	-	=O	-	$C(O)CH_3$
α-dihydrocorticosterone (**5α-DiHCORT**)	$C_{21}H_{32}O_4$	349.2373	5.9	3-keto-5α/5β-reduced steroid*	-	=O	—OH	$C(O)CH_2OH$
estriol (**E3**)	$C_{18}H_{24}O_3$	289.1798	5.0	phenolic A ring steroid	A ring	—OH	-	—OH
3α-androstanediol (**3α-Diol**)	$C_{19}H_{32}O_2$	293.2475	8.8	3-hydroxy-5α/5β-reduced steroid	-	—OH	-	—OH
7α-hydroxy DHEA (**7α-OH-DHEA**)	$C_{19}H_{28}O_3$	305.2111	5.6	Δ^5-3-hydroxysteroid‡	Δ^5	—OH	-	=O
17α-hydroxyallopregnanolone (**17α-OH-AlloP**)	$C_{21}H_{34}O_3$	335.2581	9.5	3-hydroxy-5α/5β-reduced steroid	-	—OH	-	OH + $C(O)CH_3$
androsterone (**AN**)	$C_{19}H_{30}O_2$	291.2319	9.3	non classified	Δ^1	—OH	-	=O
7ß-hydroxy DHEA (**7ß-OH-DHEA**)	$C_{19}H_{28}O_3$	305.2111	5.1	Δ^5-3-hydroxysteroid‡	Δ^5	—OH	-	=O
17ß-hydroxyallopregnanolone (**17ß-OH-AlloP**)	$C_{21}H_{34}O_3$	335.2581	9.4	3-hydroxy-5α/5β-reduced steroid	-	—OH	-	OH + $C(O)CH_3$
16α-hydroxy DHEA (**16α-OH-DHEA**)	$C_{19}H_{28}O_3$	305.2111	6.1	Δ^5-3-hydroxysteroid‡	Δ^5	—OH	-	=O
17α-hydroxypregnenolone (**17α-OH-P5**)	$C_{21}H_{32}O_3$	333.2424	8.3	Δ^5-3-hydroxysteroid	Δ^5	—OH	-	OH + $C(O)CH_3$
tetrahydro deoxycorticosterone (**THDOC**)	$C_{21}H_{34}O_3$	335.2581	8.9	3-hydroxy-5α/5β-reduced steroid	-	—OH	-	$C(O)CH_2OH$
allopregnanolone (**AlloP**)	$C_{21}H_{34}O_2$	319.2632	10.4	3-hydroxy-5α/5β-reduced steroid	-	—OH	-	$C(O)CH_3$

** also belong to the C17 alkyl side chain steroids category, ǂ also present a hydroxyl group on C7 or C16*

Fragmentation behavior of underivatized steroids

The choice of collision energy (CE) in CID-based workflows is critical for structural elucidation, as it directly governs the extent and nature of fragment ions observed in MS/MS spectra. In many studies, an intermediate CE value, typically around 30-35 eV, is selected as a practical compromise. At low CE values, fragmentation is minimal, providing limited structural information. In contrast, at high CE, extensive fragmentation can occur, leading to the formation of numerous low-mass ions that are often non-specific and poorly diagnostic of steroid substructure. When MS/MS spectra are acquired at an intermediate CE, most steroid structural categories exhibit characteristic fragmentation patterns and category-specific diagnostic ions while preserving interpretable backbone fragments that enable reliable differentiation. An example of MS/MS spectra acquired at CE 30 V for representative steroids from each structural category studied here are shown in **Figure 2** and MS/MS spectra at CE 30 V for the 33 studied steroids are shown in **Supplementary Data (Figure S3)**.

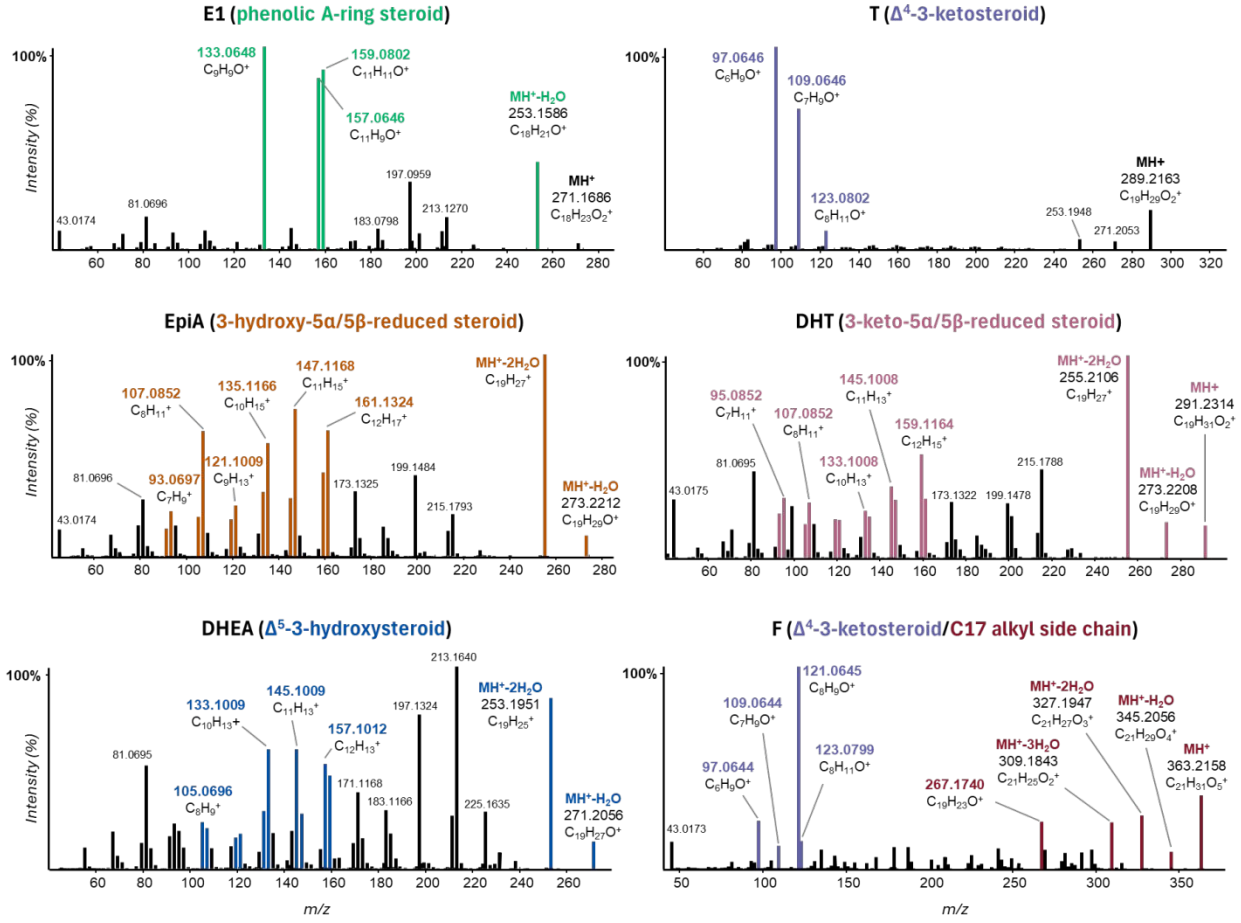

Figure 2. MS/MS fragmentation spectra acquired at CE 30 V for estrone (E1), testosterone (T), epiandrosterone (EpiA), dehydrotestosterone (DHT), dehydroepiandrosterone (DHEA) and cortisol (F) with category-specific ions highlighted.

As shown in **Figure 2**, several structural categories exhibit characteristic diagnostic fragment ions, allowing their differentiation from other categories. For example, phenolic A-ring steroids consistently generate prominent fragment ions at *m/z* 133.065, 157.065 and 159.080, the latter two reflecting a double bond (2H) either formed in the resulting fragment ions or the neutral lost. These ions are generated from a charge-directed fragmentation within the conjugated A-ring system and are highly specific to this structural motif. Δ^4-3-ketosteroids are also identifiable through the presence of diagnostic fragment ions at *m/z* 97.065, 109.065, and 123.080, originating from A-ring and A/B-ring cleavage pathways. The elemental compositions of these ions include one or more oxygen atoms. This behavior is attributed to the enhanced stability given by conjugated systems, either the fully aromatic A-ring in phenolic steroids or the α,β-unsaturated carbonyl in Δ^4-3-ketosteroids, which limit dehydration and favor the retention of the oxygen on the fragment ion. In contrast, steroids lacking such conjugation show an increased tendency toward water losses, resulting in predominantly non-oxygenated fragment ions.

This effect is clearly illustrated by comparing the MS/MS spectra of testosterone and dihydrotestosterone (DHT), differing only by the C4-C5 double bond. In the DHT spectra, fragmentation is dominated by dehydration reactions, leading to the formation of non-oxygenated ions. The resulting spectrum is considerably more complex and is characterized by numerous fragment ion pairs differing by 2 Da (2H mass differences related to a double bond either staying on the fragment ions or the neutral molecule lost). This behavior is observed across three structural categories: 3-keto-5α/5β-reduced steroids, 3-hydroxy-5α/5β-reduced steroids, and Δ^5-3-hydroxysteroids, making their differentiation based on individual fragment ions alone challenging. However, the comparison of spectra from dehydroepiandrosterone (DHEA) and epiandrosterone (EpiA) demonstrates that the presence of a hydroxyl group at C3, rather than a carbonyl group, results in a facile water loss. In these cases, the intact precursor is no longer detectable at intermediate collision energies (from CE 15 V for EpiA and CE 20 V for DHEA). In contrast, 3-keto-5α/5β-reduced steroids still have a detectable precursor ion at CE 30 V, reflecting a lower tendency for dehydration in the absence of a hydroxyl group. Accordingly, precursor ion presence, dehydration behavior, and Δ2 fragment ion pairs together constitute strong criteria for discrimination between 3-hydroxy and 3-keto reduced steroids. These differences in fragmentation behavior are also highly informative for individual compounds. For example, testosterone and dehydroepiandrosterone are isomeric species but display very distinct MS/MS spectra, underscoring the strong influence of A-ring functionality and the position of the double bond on their MS/MS behavior.

High-resolution MS/MS further enables discrimination between fragments of identical nominal mass but differing elemental composition. This can be seen by comparing estrone and DHEA spectra, where ions at nominal *m/z* 133 correspond to distinct exact masses (*m/z* 133.065 *vs.* 133.101). Such differences highlight the necessity of high-resolution MS/MS for accurate fragment assignment, as these ions would be indistinguishable using low resolution approaches, such as traditional MRM acquisition on triple quadrupole platforms. Finally, certain steroid categories do not have unique diagnostic fragment ions but are instead characterized by specific

neutral losses. For example, C17 alkyl side chain steroids, often presents neutral losses corresponding to the side-chain cleavage, along with consecutive water losses. These fragmentations reflect the presence of many oxygen atoms and a side chain in their structures. Based on their presence in multiple steroids within the same category, a list of diagnostic ions and neutral losses is compiled in Table 2, along with the associated category and collision energy range where the ions or NL can be observed.

Table 2: Diagnostic ions and neutral losses of underivatized steroids

Formula	*m/z (or Da)*	Fragmentation type	CE range (V)	Associated steroid class	Diagnostic value
$C_7H_7^+$	91.054	A ring cleavage	30-60	5α/5β-reduced / 3-hydroxy steroid	supportive
$C_7H_9^+$	93.070	A ring cleavage	30-60	5α/5β-reduced / 3-hydroxy steroid	supportive
$C_7H_{11}^+$	95.086	A ring cleavage	25-60	5α/5β-reduced / 3-hydroxy steroid	supportive
$C_6H_9O^+$	97.065	A ring cleavage	25-60	Δ4-3-ketosteroid	class-specific
$C_8H_9^+$	105.070	B ring cleavage	20-60	5α/5β-reduced / 3-hydroxy steroid	supportive
$C_7H_7O^+$	107.049	B ring cleavage	20-60	Δ4-3-ketosteroid / phenolic A ring	class-specific
$C_8H_{11}^+$	107.086	B ring cleavage	20-60	5α/5β-reduced / 3-hydroxy steroid	supportive
$C_7H_9O^+$	109.065	B ring cleavage	20-60	Δ4-3-ketosteroid	class-specific
$C_9H_{11}^+$	119.086	B ring cleavage	20-60	5α/5β-reduced / 3-hydroxy steroid	supportive
$C_9H_{13}^+$	121.101	B ring cleavage	20-60	5α/5β-reduced / 3-hydroxy steroid	supportive
$C_8H_9O^+$	121.065	B ring cleavage	25-60	Δ4-3-ketosteroid	class-specific
$C_8H_{11}O^+$	123.080	B ring cleavage	25-60	Δ4-3-ketosteroid	class-specific
$C_{10}H_{11}^+$	131.086	B ring cleavage	25-60	5α/5β-reduced / 3-hydroxy steroid	supportive
$C_9H_9O^+$	133.065	B ring cleavage	15-60	phenolic A ring steroid	class-specific
$C_{10}H_{13}^+$	133.101	B ring cleavage	20-60	5α/5β-reduced / 3-hydroxy steroid	supportive
$C_{10}H_{15}^+$	135.117	B ring cleavage	20-60	5α/5β-reduced / 3-hydroxy steroid	supportive
$C_{11}H_{13}^+$	145.101	C ring cleavage	20-60	5α/5β-reduced / 3-hydroxy steroid	supportive
$C_{11}H_{15}^+$	147.117	C ring cleavage	20-60	5α/5β-reduced / 3-hydroxy steroid	supportive
$C_{11}H_9O^+$	157.065	C ring cleavage	15-60	phenolic A ring steroid	class-specific
$C_{11}H_{11}O^+$	159.080	C ring cleavage	15-60	phenolic A ring steroid	class-specific
$C_{12}H_{15}^+$	159.117	C ring cleavage	20-60	5α/5β-reduced / 3-hydroxy steroid	supportive
$C_{12}H_{17}^+$	161.132	C ring cleavage	20-55	5α/5β-reduced / 3-hydroxy steroid	supportive
$C_{11}H_{15}O^+$	163.112	C ring cleavage	25-60	Δ4-3-ketosteroid	class-specific
H_2O	-18.012	water loss	10-40	-	non-specific
$C_2H_3O_2$	-60.021	side chain loss (C17-C20)	25-35	C17 alkyl side chain	class-specific
C_2H_3O	-44.026	side chain loss (C17-C20)	25-35	C17 alkyl side chain	class-specific

As discussed, collision energy in CID experiments has a strong influence on fragmentation behavior. This effect is evident for steroids that possess a rigid and highly stable carbon backbone and therefore do not undergo extensive fragmentation at low energy. As a result, certain diagnostic fragment ions are only formed or become detectable at specific collision energy windows, either at lower or higher CE values. In this study, multiple CE values ranging from 10 to 60 V were applied to study steroid fragmentation. To facilitate comparison of fragment ion behavior across collision energies, fragments signals were normalized by calculating their relative intensity using the precursor ion intensity measured at the lowest CE (10 V) as a reference. Using the diagnostic fragment ions listed in **Table 2**, breakdown curves were constructed to illustrate the evolution of fragment ion intensities as a function of CE. Representative breakdown curves for one steroid from each structural category are shown in **Figure 3**, while all fragment ion matrices, used for plotting the breakdown curves, can be found in **Supplementary Data (Table S2)**.

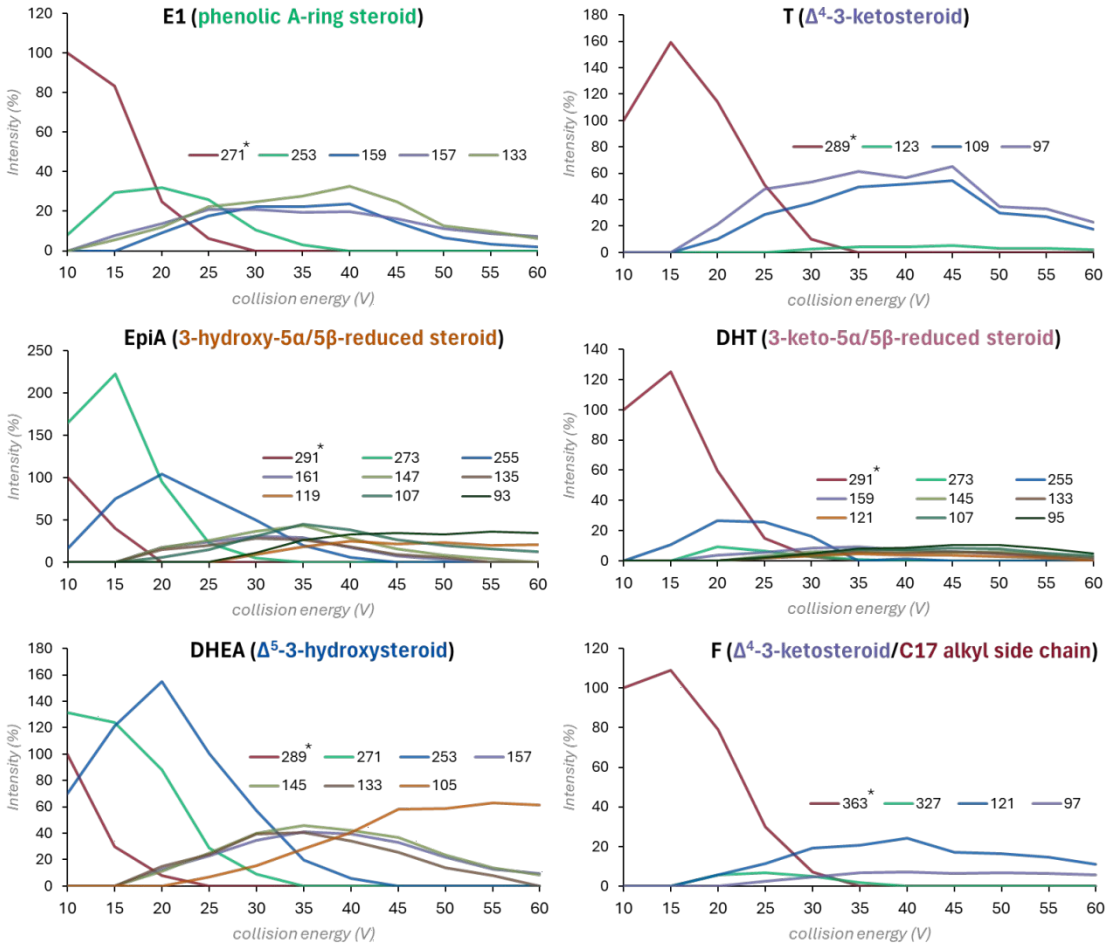

Figure 3. Breakdown curves showing precursor and fragment ions of interest from CE 10-60 V for estrone (E1), testosterone (T), epiandrosterone (EpiA), dehydrotestosterone (DHT), dehydroepiandrosterone (DHEA) and cortisol (F), as representative steroids from each class studied

For most compounds, the precursor ion intensity was slightly higher at CE 15 or 20V than at CE 10 V. This behavior reflects the fact that precursor signal intensity is influenced not only by fragmentation but also by ion transmission efficiency and internal energy distribution within the collision cell. At very low CE, ion focusing, and transmission in a TOF based analyzer can be less efficient, leading to reduced signal intensity. A small increase in collision energy thus can show enhanced ion transmission, while the precursor ion remains largely intact, resulting in an apparent increase in precursor intensity.

Breakdown curves further reflect the characteristic fragmentation behavior of each structural category. For example, estrone, testosterone, and cortisol generate a limited number of diagnostic fragment ions, and the intact precursor ion remains detectable up to approximately CE 35 V. For estrone and testosterone, the major diagnostic ions reach maximum relative intensity between CE 30 and 45 V before gradually decreasing at higher collision energies, although they remain detectable even at CE 60 V. This behavior indicates that once these ions are formed, they are relatively stable and persist across a wide CE range.

For 3-hydroxy-containing steroids, such as dehydroepiandrosterone (DHEA) and epiandrosterone (EpiA), fragment ions corresponding to a water loss are observed with high relative intensities. This behavior is consistent with the previously discussed behavior of hydroxyl groups, which promotes facile dehydration under CID conditions. This can be explained by the greater stability of the dehydrated species relative to the intact precursor. Finally, for 3-hydroxy steroids, the intact precursor ion is detectable only at low collision energies and is not detectable above CE 20 V. This rapid loss of the precursor ion provides an additional, CE-dependent diagnostic feature that can be exploited to support structural assignment and confirm compound identity.

Fragmentation behavior of Girard P derivatized steroids

As discussed earlier, chemical derivatization is a widely used sample preparation strategy for LC-MS analysis of steroids. Derivatization reagents can also introduce an easily ionizable moiety or a permanent charge, with the aim of enhancing the detectability of otherwise poorly ionizing steroids. In addition to improving ionization efficiency, derivatization also impacts the physicochemical properties of the analytes, resulting in modified chromatographic behavior. In this study, a commonly used hydrazine-based reagent, Girard P (GP), was employed to derivatize the investigated steroids, by adding a hydrazine onto the carbonyls of the steroids, forming a hydrazone derivative. An example for the derivatization reaction for testosterone is shown in **Supplementary Data (Figure S4).** After this reaction, the steroid–GP conjugates carry a permanent positive charge and are observed directly as M^+ forms. For steroids having two potential derivatization sites, the doubly derivatized species (as doubly charged ions) were also investigated, however, none were detected. A detailed list of all the derivatized steroids with their associated retention times, masses, derivatizable groups and increased response factor can be found in **Table 3.** The effects on detectability and chromatographic separation of GP-

derivatized steroids, were seen to be quite dependent on the structure of the steroid, as illustrated in **Figure 4**.

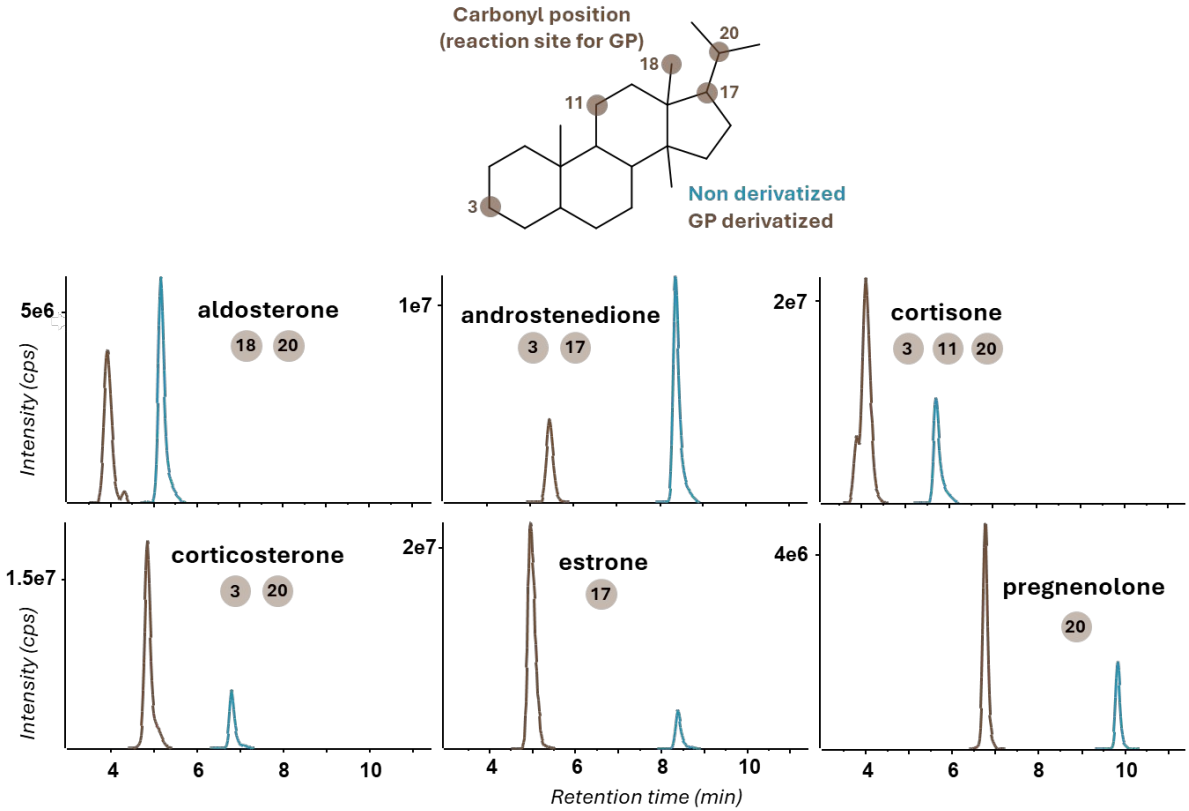

Figure 4: Extracted ion chromatograms for representative underivatized steroids and their corresponding Girard P derivatized version, with potential reaction site

In some cases, GP-derivatized steroids exhibit higher signal intensity than their underivatized counterparts, however this is not always the case. This enhancement can be attributed to the presence of the quaternary ammonium introduced by the GP reagent, thereby facilitating the "ionization" step and improving detectability under ESI conditions. Changes in signal intensity following Girard P derivatization were observed, with variable signal enhancements, as illustrated in **Figure 4** and summarized in **Table 3**. This could also in part be due to differences in derivatization yield depending on the carbonyl site targeted.

Table 3: Girard P derivatized steroids with their formulae, exact masses, retention times, position of possible derivatization and relative increase in peak areas compared to their underivatized counterparts

Name	Formula	Exact mass (M^+)	RT (min)	carbonyl position	Peak area ratio GP/UD
E1-GP	$C_{25}H_{30}O_2N_3$	404.2333	5.0	C17	**8.6**
T-GP	$C_{26}H_{36}O_2N_3$	422.2802	5.3*	C3	2.0
EpiA-GP	$C_{26}H_{38}O_2N_3$	424.2959	5.2	C17	**32.5**
P5-GP	$C_{28}H_{40}O_2N_3$	450.3115	6.8	C20	2.4
11α-OHP-GP	$C_{28}H_{38}O_3N_3$	464.2908	5.5*	C3, C20	2.6
E-GP	$C_{28}H_{36}O_5N_3$	494.2650	4.1*	C3, C11, C20	1.6
DHEA-GP	$C_{26}H_{36}O_2N_3$	422.2802	5.0	C17	**50.4**
P4-GP	$C_{28}H_{38}O_2N_3$	448.2959	7.1*	C3, C20	2.6
11-DOC-GP	$C_{28}H_{38}O_3N_3$	464.2908	5.9*	C3, C20	2.7
11-DHC-GP	$C_{28}H_{36}O_4N_3$	478.2700	4.7*	C3, C11, C20	5.8
CORT-GP	$C_{28}H_{38}O_4N_3$	480.2857	4.9*	C3, C20	3.6
F-GP	$C_{28}H_{38}O_5N_3$	496.2806	4.2*	C3, C20	4.9
5ß-DiHP4-GP	$C_{28}H_{40}O_2N_3$	450.3115	8.3*	C3, C20	0.0
5ß-DiHCORT-GP	$C_{28}H_{40}O_4N_3$	482.3013	4.9*	C3, C20	2.3
ALD-GP	$C_{28}H_{36}O_5N_3$	494.2650	3.9*	C3, C18, C20	0.8
A4-GP	$C_{26}H_{34}O_2N_3$	420.2646	5.4*	C3, C17	0.5
11-KT -GP	$C_{26}H_{34}O_3N_3$	436.2595	4.4*	C3, C11	3.0
5α-DiHP4-GP	$C_{28}H_{40}O_2N_3$	450.3115	7.5	C3, C20	0.0
5α-DiHCORT-GP	$C_{28}H_{40}O_4N_3$	482.3013	4.3*	C3, C20	1.9
7α-OH-DHEA-GP	$C_{26}H_{36}O_3N_3$	438.2751	3.8	C17	**<u>60.5</u>**
17α-OH-AlloP-GP	$C_{28}H_{42}O_3N_3$	468.3221	6.3	C20	**11.9**
AN-GP	$C_{26}H_{38}O_2N_3$	424.2959	6.5	C17	**23.5**
7ß-OH-DHEA-GP	$C_{26}H_{36}O_3N_3$	438.2751	3.1	C17	<u>3.9</u>
17ß-OH-AlloP-GP	$C_{28}H_{42}O_3N_3$	468.3221	6.4	C20	6.6
16α-OH-DHEA-GP	$C_{26}H_{36}O_3N_3$	438.2751	4.5	C17	**<u>26.0</u>**
17α-OH-P5-GP	$C_{28}H_{38}O_3N_3$	466.3064	5.2	C20	<u>6.5</u>
AlloP-GP	$C_{28}H_{42}O_2N_3$	452.3272	7.3	C20	0.0

** present as a double peak, <u>underlined</u> ratios were calculated using water loss precursors of underivatized steroids*

Despite many advantages, chemical derivatization also presents several limitations. Steroids typically contain only carbonyl or hydroxyl functional groups, and reagents targeting these moieties often will also react with many other metabolites present in complex biological samples and, consequently, can yield a significantly increased background noise in the resulting analysis, having a potential important matrix effect. Furthermore, the addition of a derivatization group substantially alters the MS/MS spectra, meaning that the resulting fragmentation patterns are often less informative for structural elucidation, as shown for testosterone or dehydroepiandrosterone. As shown in **Figure 5A**, when a medium CE (30 V) is applied, MS/MS

spectra are dominated by fragment ions originating from the Girard P reagent. These fragments correspond to cleavage of the pyridinium cycle, cleavage of the hydrazone linkage connecting the steroid to the GP reagent, or cleavage of the amide bond of the GP. Fragmentation at low to intermediate collision energies is largely restricted to the GP moiety. At higher energies, however, the fragmentation spectra exhibit structurally informative fragments, as shown at CE of 60 V in **Figure 5B**, where diagnostic ions are present to help differentiate isomeric steroids, testosterone-GP and DHEA-GP.

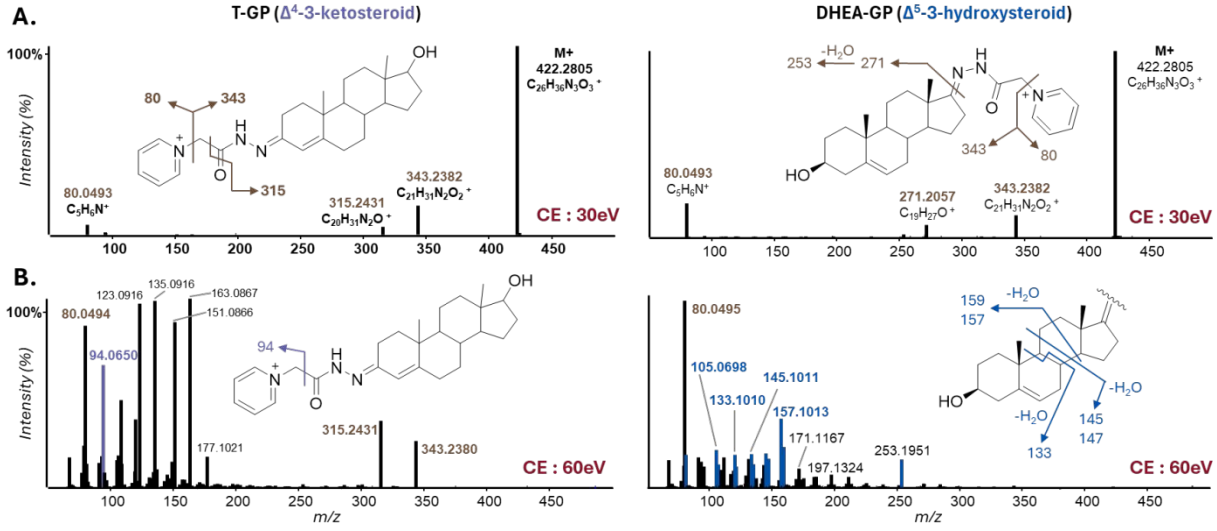

Figure 5: MS/MS spectra of Girard P derivatized testosterone (T-GP) and dehydroepiandrosterone (DHEA-GP) at CE 30 V (A) and 60 V (B)

At most collision energies, testosterone-GP does not exhibit fragment ions that can be directly associated with the steroid backbone. However, a distinct fragment ion at *m/z* 94.065 becomes prominent at CE of 60 V. This ion corresponds to cleavage of the pyridinium moiety with a methyl substituent still attached and is observed exclusively and reproducibly for 3-keto steroids containing an α,β-unsaturated carbonyl system. Importantly, this ion was not detected for any other steroid structural category, further emphasizing the critical role of the conjugated carbonyl system in CID fragmentation. This case highlights the importance of CE selection for accessing class-specific diagnostic information.

Dehydroepiandrosterone (DHEA), which is isomeric with testosterone but lacks an α,β-unsaturated carbonyl, does not generate this fragment. DHEA-GP can also be differentiated from its isomer T-GP through the formation of structural diagnostic ions at *m/z* 271 at intermediate CE and *m/z* 253 at higher CE (as shown in Figure 5). A recent study showed that GP-derivatized steroids can also be fragmented using electron-activated dissociation (EAD), offering an alternative dissociation strategy to CID[33], however EAD usually produces lower fragmentation yields than CID in general[34,35]. The CID MS/MS spectrum of DHEA-GP at higher CE (shown in Figure

5B) displays multiple fragment ions that are the same as the ones observed for its underivatized compound, which is not the case for many other GP derivatized steroids. This indicates that once the GP moiety is fully dissociated at elevated CE, fragmentation of the steroid backbone can occur in a similar way as the native steroid. In addition, the DHEA-GP produces a fragment ion at *m/z* 157.101, observed exclusively for Δ^5-3-hydroxysteroids. This ion therefore constitutes a useful diagnostic marker for differentiating this structural category from other steroids that exhibit similar fragmentation behavior in their underivatized form. A list of the main fragment ions and neutral losses associated with Girard P derivatized steroids is compiled in **Table 4**.

Table 4: Fragment ions and neutral losses of interest for GP-derivatized steroids

Formula	*m/z*	Fragmentation type	CE range (V)	Associated steroids class	Diagnostic value
$C_5H_6N^+$	80.049	Girard P cleavage	25-60	-	non-specific
$C_6H_8N^+$	94.065		40-60	Δ4-3-ketosteroids	**class-specific**
$C_{12}H_{13}^+$	157.101	underivatized steroid fragments	40-60	Δ5-3-hydroxysteroids	**class-specific**
$C_{11}H_{13}^+$	145.101		40-60	Δ5-3-hydroxysteroids	**class-specific**
$C_{10}H_{13}^+$	133.101		40-60	Δ5-3-hydroxysteroids	**class-specific**
$C_8H_9^+$	105.070		40-60	Δ5-3-hydroxysteroids	**class-specific**
C_5H_5N	-79.042	neutral loss related to GP moiety	25-60	-	non-specific
C_6H_5NO	-107.037		30-60	-	non-specific
$C_7H_9N_3O$	-151.075		30-60	-	non-specific

Conclusion

This study investigated the fragmentation behavior of 33 endogenous steroids using LC-MRM^{HR} acquisition on a QqTOF platform at a range of collision energies, for both native and Girard P derivatized steroids. By grouping steroids into structural categories based on A-ring functionality and oxidation state, clear fragmentation trends were observed. Phenolic and Δ^4-3-ketosteroids generated oxygen containing diagnostic ions and reduced and Δ^5-steroids displayed highly complex spectra dominated by dehydration and characteristic Δ2 fragment ion pairs. Collision energy was shown to strongly impact fragmentation spectra, with both precursor presence/absence and fragment ion formation exhibiting strong CE dependence. Breakdown curves demonstrated that diagnostic ions often emerge within defined CE windows, while excessive fragmentation at high CE can obscure structural information. These results highlight the importance of CE setting for comprehensive steroid structural characterization. Girard P derivatization further expanded the structural information accessible by CID MS/MS. At high collision energy, selective GP-derived diagnostic ions and, in some cases, recovery of backbone-like fragmentation enabled discrimination of closely related isomers. These findings demonstrate that GP derivatization can provide complementary structural information in addition to

modifying chromatographic behavior and sensitivity. All these observations can be useful in determining the category of an unknown steroid, in the case of untargeted analysis of complex biological samples, and even some structural characteristics, such as carbonyl position. Isomeric species could be differentiated by derivatization or by altering CID conditions. All these results have been summarized in a decision tree shown in **Figure 6**.

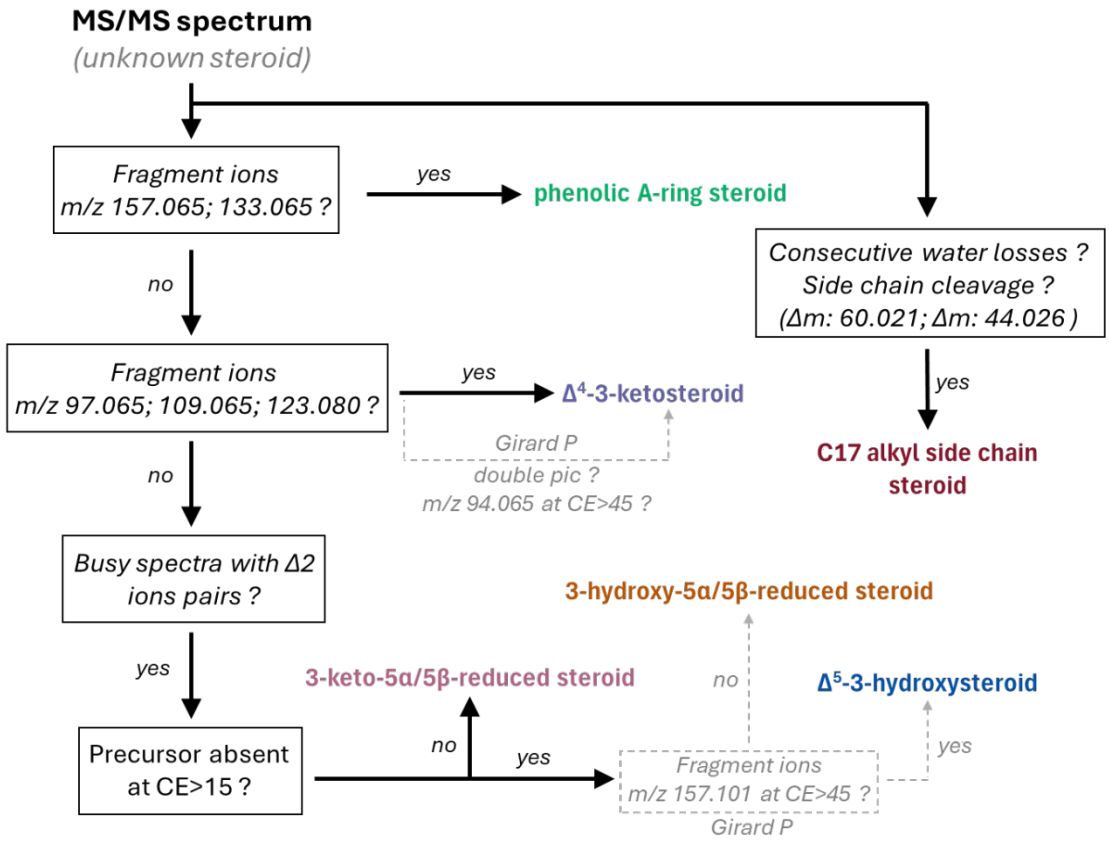

Figure 6: Decision tree for structural characterization of steroids using HR-MS/MS data

Abbreviations

CE: Collision energy (*or* collision-offset voltage)

CID: Collision induced dissociation

ESI: Electrospray ionization

GP: Girard P

HR-MS/MS: High resolution tandem mass spectrometry

microLC: microflow liquid chromatography

MRM: multiple reaction monitoring

NL: neutral loss

QqTOF: quadrupole time-of-flight

RT: retention time

UD: underivatized

Conflict of interest statement

The authors have no conflict of interest to declare.

Author contributions

N.G. (Conceptualization, Investigation, Methodology, Writing – original draft)

L.S. (Conceptualization, Methodology, Funding acquisition, Supervision, Writing – review & editing)

Funding

This work was supported by a Discovery Grant from the Natural Sciences and Engineering Research Council of Canada (NSERC; Grant No. 2026-04684). The authors also acknowledge instrumental platform support from the CERMO-FC (*Centre d'Excellence de Recherche sur les Maladies Orphelines – Fondation Courtois*) mass spectrometry platform. L.S. is the recipient of an institutional strategic research chair in Bioanalytical Chemistry at UQAM.

Data availability

Data can be made available through directly contacting the corresponding author.

Figure legends

Figure 1: Structural categories of endogenous steroids studied in this work

Figure 2: MS/MS fragmentation spectra acquired at CE 30 V for estrone (E1), testosterone (T), epiandrosterone (EpiA), dehydrotestosterone (DHT), dehydroepiandrosterone (DHEA) and cortisol (F) with category-specific ions highlighted.

Figure 3: Breakdown curves showing precursor and fragment ions of interest from CE 10-60 V for estrone (E1), testosterone (T), epiandrosterone (EpiA), dehydrotestosterone (DHT), dehydroepiandrosterone (DHEA) and cortisol (F), as representative steroids from each class studied

Figure 4: Extracted ion chromatograms for representative underivatized steroids and their corresponding Girard P derivatized version, with potential reaction site

Figure 5: MS/MS spectra of Girard P derivatized testosterone (T-GP) and dehydroepiandrosterone (DHEA-GP) at CE 30 (A) and 60 V (B)

Figure 6: Decision tree for structural characterization of steroids using HR-MS/MS data

References

(1) Litwack, G. *Chapter 2 - Steroid hormones: chemistry, biosynthesis, and metabolism*. Editor: Litwack, G. *Hormones (Fourth Edition)*, Academic Press, **2022**, 29-55. https://doi.org/10.1016/B978-0-323-90262-5.00018-4.

(2) Barreira, J. C. M.; Ferreira, I. C. F. R. Steroids in Natural Matrices. In *Biotechnology of Bioactive Compounds*; John Wiley & Sons, Ltd, **2015**; pp 395–431. https://doi.org/10.1002/9781118733103.ch16.

(3) Biellmann, J.-F. Enantiomeric Steroids: Synthesis, Physical, and Biological Properties. *Chem. Rev.* **2003**, *103* (5), 2019–2034. https://doi.org/10.1021/cr020071b.

(4) Tsuchiya, H.; Mizogami, M. Discrimination of Stereoisomers by Their Enantioselective Interactions with Chiral Cholesterol-Containing Membranes. *Molecules* **2018**, *23* (1), 49. https://doi.org/10.3390/molecules23010049.

(5) Covey, D. F. *Ent*-Steroids: Novel Tools for Studies of Signaling Pathways. *Steroids* **2009**, *74* (7), 577–585. https://doi.org/10.1016/j.steroids.2008.11.019.

(6) Zarzycki, P. K.; Wierzbowska, M.; Lamparczyk, H. The Influence of Temperature on the Multiple Separation of Estrogenic Steroids Using Mobile Phases Modified with β-Cyclodextrin in High-Performance Liquid Chromatography. *Journal of Pharmaceutical and Biomedical Analysis* **1997**, *15* (9), 1281–1287. https://doi.org/10.1016/S0731-7085(96)01974-7.

(7) Kummer, M.; Palme, H.-J.; Werner, G. Resolution of Enantiomeric Steriod by High-Performance Liquid Chromatography on Chiral Stationary Phases. *Journal of Chromatography A* **1996**, *749* (1), 61–68. https://doi.org/10.1016/0021-9673(96)00364-0.

(8) Shimada, K.; Mitamura, K.; Higashi, T. Gas Chromatography and High-Performance Liquid Chromatography of Natural Steroids. *Journal of Chromatography A* **2001**, *935* (1), 141–172. https://doi.org/10.1016/S0021-9673(01)00943-8.

(9) Hernández-Mesa, M.; Monteau, F.; Le Bizec, B.; Dervilly-Pinel, G. Potential of Ion Mobility-Mass Spectrometry for Both Targeted and Non-Targeted Analysis of Phase II Steroid Metabolites in Urine. *Analytica Chimica Acta: X* **2019**, *1*, 100006. https://doi.org/10.1016/j.acax.2019.100006.

(10) Li, Y.; Qin, Y.; Wei, S.; Ling, L.; Ding, C.-F. Differentiation of Steroid Isomers by Steroid Analogues Adducted Trapped Ion Mobility Spectrometry-Mass Spectrometry. *Anal Bioanal Chem* **2024**, *416* (1), 313–319. https://doi.org/10.1007/s00216-023-05019-5.

(11) Rister, A. L.; Dodds, E. D. Liquid Chromatography-Ion Mobility Spectrometry-Mass Spectrometry Analysis of Multiple Classes of Steroid Hormone Isomers in a Mixture. *Journal of Chromatography B* **2020**, *1137*, 121941. https://doi.org/10.1016/j.jchromb.2019.121941.

(12) Davis, D. E. Jr.; Leaptrot, K. L.; Koomen, D. C.; May, J. C.; Cavalcanti, G. de A.; Padilha, M. C.; Pereira, H. M. G.; McLean, J. A. Multidimensional Separations of Intact Phase II Steroid Metabolites Utilizing LC–Ion Mobility–HRMS. *Anal. Chem.* **2021**, *93* (31), 10990–10998. https://doi.org/10.1021/acs.analchem.1c02163.

(13) Rister, A. L.; Dodds, E. D. Steroid Analysis by Ion Mobility Spectrometry. *Steroids* **2020**, *153*, 108531. https://doi.org/10.1016/j.steroids.2019.108531.

(14) Ray, J. A.; Kushnir, M. M.; Yost, R. A.; Rockwood, A. L.; Wayne Meikle, A. Performance Enhancement in the Measurement of 5 Endogenous Steroids by LC–MS/MS Combined with Differential Ion Mobility Spectrometry. *Clinica Chimica Acta* **2015**, *438*, 330–336. https://doi.org/10.1016/j.cca.2014.07.036.

(15) Higashi, T.; Shimada, K. Derivatization of Neutral Steroids to Enhance Their Detection Characteristics in Liquid Chromatography–Mass Spectrometry. *Anal Bioanal Chem* **2004**, *378* (4), 875–882. https://doi.org/10.1007/s00216-003-2252-z.

(16) Marcos, J.; Pozo, O. J. Derivatization of Steroids in Biological Samples for GC–MS and LC–MS Analyses. *Bioanalysis* **2015**, *7* (19), 2515–2536. https://doi.org/10.4155/bio.15.176.
(17) Yan, Z.; Cheng, C.; Liu, S. Applications of Mass Spectrometry in Analyses of Steroid Hormones. In *LC-MS in Drug Bioanalysis*; Xu, Q. A., Madden, T. L., Eds.; Springer US: Boston, MA, 2012; pp 251–286. https://doi.org/10.1007/978-1-4614-3828-1_10.
(18) Šimková, M.; Kolátorová, L.; Dražar, P.; Vítků, J. An LC-MS/MS Method for the Simultaneous Quantification of 32 Steroids in Human Plasma. *Journal of Chromatography B* **2022**, *1201–1202*, 123294. https://doi.org/10.1016/j.jchromb.2022.123294.
(19) Athanasiadou, I.; Angelis, Y. S.; Lyris, E.; Georgakopoulos, C.; Athanasiadou, I.; Georgakopoulos, C. Chemical Derivatization to Enhance Ionization of Anabolic Steroids in LC-MS for Doping-Control Analysis. *TrAC Trends in Analytical Chemistry* **2013**, *42*, 137–156. https://doi.org/10.1016/j.trac.2012.10.003.
(20) Penning, T. M.; Lee, S.-H.; Jin, Y.; Gutierrez, A.; Blair, I. A. Liquid Chromatography–Mass Spectrometry (LC–MS) of Steroid Hormone Metabolites and Its Applications. *The Journal of Steroid Biochemistry and Molecular Biology* **2010**, *121* (3), 546–555. https://doi.org/10.1016/j.jsbmb.2010.01.005.
(21) Velosa, D. C.; Dunham, A. J.; Rivera, M. E.; Neal, S. P.; Chouinard, C. D. Improved Ion Mobility Separation and Structural Characterization of Steroids Using Derivatization Methods. *J. Am. Soc. Mass Spectrom.* **2022**, *33* (9), 1761–1771. https://doi.org/10.1021/jasms.2c00164.
(22) Su, M.; Drotleff, B.; Janker, T.; Bürger, Z.; Kimmig, A.-C. S.; Derntl, B.; Lämmerhofer, M. Quantification of Endogenous Steroids and Hormonal Contraceptives in Human Plasma via Surrogate Calibration and UHPLC-MS/MS. *Anal. Chem.* **2025**, *97* (25), 13496–13503. https://doi.org/10.1021/acs.analchem.5c01912.
(23) Son, H. H.; Yun, W. S.; Cho, S.-H. Development and Validation of an LC-MS/MS Method for Profiling 39 Urinary Steroids (Estrogens, Androgens, Corticoids, and Progestins). *Biomedical Chromatography* **2020**, *34* (2), e4723. https://doi.org/10.1002/bmc.4723.
(24) An LC/MS/MS Method for Analyzing the Steroid Metabolome with High Accuracy and from Small Serum Samples. *J Lipid Res* **2020**, *61* (4), 580–586. https://doi.org/10.1194/jlr.D119000591.
(25) Gjorgoska, M.; Rižner, T. L. Simultaneous Measurement of 17 Endogenous Steroid Hormones in Human Serum by Liquid Chromatography-Tandem Mass Spectrometry without Derivatization. *The Journal of Steroid Biochemistry and Molecular Biology* **2024**, *243*, 106578. https://doi.org/10.1016/j.jsbmb.2024.106578.
(26) Xing, S.; Jiao, Y.; Salehzadeh, M.; Soma, K. K.; Huan, T. SteroidXtract: Deep Learning-Based Pattern Recognition Enables Comprehensive and Rapid Extraction of Steroid-Like Metabolic Features for Automated Biology-Driven Metabolomics. *Anal. Chem.* **2021**, *93* (14), 5735–5743. https://doi.org/10.1021/acs.analchem.0c04834.
(27) Mohanty, I.; Xing, S.; Castillo, V.; Agongo, J.; Patan, A.; El Abiead, Y.; Mannochio-Russo, H.; Gonçalves Nunes, W. D.; Zemlin, J.; Mizrahi, I.; Siegel, D.; Wang, M.; Hagey, L. R.; Dorrestein, P. C. MS/MS Mass Spectrometry Filtering Tree for Bile Acid Regio- and Stereoisomer Annotation. *Anal. Chem.* **2026**, *98* (6), 4571–4584. https://doi.org/10.1021/acs.analchem.5c05677.
(28) Böcker, S.; Letzel, M. C.; Lipták, Z.; Pervukhin, A. SIRIUS: Decomposing Isotope Patterns for Metabolite Identification†. *Bioinformatics* **2009**, *25* (2), 218–224. https://doi.org/10.1093/bioinformatics/btn603.
(29) Penning, T. M.; Chen, M.; Jin, Y. Promiscuity and Diversity in 3-Ketosteroid Reductases. *J Steroid Biochem Mol Biol* **2015**, *151*, 93–101. https://doi.org/10.1016/j.jsbmb.2014.12.003.
(30) Pozo, O. J.; Lootens, L.; Van Eenoo, P.; Deventer, K.; Meuleman, P.; Leroux-Roels, G.; Parr, M. K.; Schänzer, W.; Delbeke, F. T. Combination of Liquid-Chromatography Tandem Mass Spectrometry

in Different Scan Modes with Human and Chimeric Mouse Urine for the Study of Steroid Metabolism. *Drug Testing and Analysis* **2009**, *1* (11–12), 554–567. https://doi.org/10.1002/dta.56.

(31) Schiffer, L.; Shaheen, F.; Gilligan, L. C.; Storbeck, K.-H.; Hawley, J.; Keevil, B. G.; Arlt, W.; Taylor, A. E. Multi-Steroid Profiling by uPLC-MS/MS with Post-Column Infusion of Ammonium Fluoride. medRxiv March 9, 2022, p 2022.03.08.22271681. https://doi.org/10.1101/2022.03.08.22271681.

(32) Chen, M.; Penning, T. M. 5β-Reduced Steroids and Human Δ4-3-Ketosteroid 5β-Reductase (AKR1D1). *Steroids* **2014**, *83*, 17–26. https://doi.org/10.1016/j.steroids.2014.01.013.

(33) Tian, T.; Cheng, H.; Zhao, X. Differentiation of Steroid Isomers via Derivatization and Electron-Activated Dissociation Tandem Mass Spectrometry. *Anal Bioanal Chem* **2025**. https://doi.org/10.1007/s00216-025-06258-4.

(34) Molina, H.; Matthiesen, R.; Kandasamy, K.; Pandey, A. Comprehensive Comparison of Collision Induced Dissociation and Electron Transfer Dissociation. *Anal. Chem.* **2008**, *80* (13), 4825–4835. https://doi.org/10.1021/ac8007785.

(35) Che, P.; Davidson, J. T.; Kool, J.; Kohler, I. Electron Activated Dissociation - a Complementary Fragmentation Technique to Collision-Induced Dissociation for Metabolite Identification of Synthetic Cathinone Positional Isomers. *Analytica Chimica Acta* **2023**, *1283*, 341962. https://doi.org/10.1016/j.aca.2023.341962.